Pergamon

Int. J. Heat Mass Transfer. Vol. 39, No. 15, pp. 3273–3286, 1996

0017-9310/96 $15.00 + 0.00

0017-9310(95)00400-9

A computationally efficient procedure for calculating gas radiative properties using the exponential wide band model

N. LALLEMANT and R. WEBER

International Flame Research Foundation, P.O. Box 10000, 1970 CA IJmuiden, The Netherlands

(*Received* 14 *February* 1994 *and in final form* 11 *July* 1995)

Abstract—A procedure to optimize the radiative property calculations of gas-mixtures using the exponential wide band model (EWBM) is described in this paper. The procedure is applicable to any nitrogen-gas mixtures containing H_2O, CO_2, CH_4, CO, SO_2, NO, C_2H_2, N_2O and NH_3. The use of this procedure in calculating the total emissivity of H_2O–CO_2 mixtures yields computational times comparable to those required by conventional emissivity correlations. The generality of the EWBM, along with minimized computational requirements, makes the procedure very attractive for incorporation into CFD codes for flame calculations. The coupling of the EWBM with classical solution methods of the RTE is discussed.

1. INTRODUCTION

Much of the current work on the modeling of industrial flames using computational fluid dynamic (CFD) codes still apply the sum of gray gases models (SGGM) [1, 2] or polynomial approximations [3, 4] to predict the total radiative properties of the absorbing gaseous phase. The primary reason underlying the development of these approximate models stemmed from the necessity to optimize the computation of total radiative properties of gases by avoiding the recourse to spectral calculations. The success encountered by these models in the mathematical modeling of flames is greatly attributed to their mathematical simplicity and their ability to simulate reasonably well the non-grayness of gases in a range of temperature and partial pressure that usually covers most furnace applications. However, all these empirical models are limited to total emissivity calculations of the volumes of homogeneous gas whose characteristic sizes are greater than about one centimeter. Recent advances in flame modeling including NO_x predictions indicate that accurate predictions of the flame front can only be accomplished using very fine computational grids. For example, in order to resolve the near burner zone (NBZ) properties of 2 MW natural gas (NG) flames, it is necessary to resort to computational cells as small as 0.5 mm [5], which is beyond the applicability domain of most of the existing emissivity correlations [6]. Moreover, in recent years, the industry has shown an increasing interest for high pressure combustion systems, either for thermodynamic reasons (e.g. gas turbines), combustion process intensification (e.g. pressurized fluidized beds) or to shift the kinetics in a desirable direction (e.g. ammonia production process plants). It is then clear that the total emissivity models which are presently used in most CFD codes and which are limited to total emissivity and absorptivity calculations at atmospheric pressure, will have to be replaced by more general models.

Although there exist no mathematical constraints why existing SGGM or polynomial approximations could not be generalized to cover a wider path length-range and broader pressure conditions, it is evident that the development of such models would require more complex mathematical formulations. Even then, the SGGM and polynomial correlations would remain limited to emissivity calculations of at most two emitting/absorbing gas species having common overlapping bands. The generalization of these emissivity models to mixtures of more than two gas species having common overlapping bands is to the authors' viewpoint beyond the reach of such models.

It is very doubtful that either polynomial correlations or sum of gray gases models will ever reach the accuracy and generality of the narrow band models (NBM) [7] or the exponential wide band model (EWBM) [8–12]. In CFD modeling of flames, the generality of radiative property models is an important factor to consider. To date, in view of the storage and speed capabilities of present computers, it is quite generally accepted that models such as the NBM or the EWBM are not suitable for CFD flame modeling. The NBM requires excessive computational times. Although the EWBM could potentially be applied, it is avoided in CFD codes mainly because of the apparent complexity of the model mathematical formulation and the belief that it requires prohibitive CPU times.

In the present paper, it is first shown how calculations using the exponential wide band model (EWBM) [8–12] can be optimized to reach computational times comparable to that of most emissivity correlations. The procedure presented herein is then

NOMENCLATURE

a_k	fitting polynomial coefficients
C_2	second Planck constant
d	line spacing
e	e = 2.178 281...
E	blackbody emissive power
f	fraction of blackbody radiation
g_k	degeneracy
k_v	mass absorption coefficient
L	path length
m	number of fundamental bands
P_t	total pressure
P_e	equivalent pressure
S_k	analytical function (see note 2 of Table 1 for the definition)
T	temperature
u_k	dimensionless group given by equation (2)
v_k	vibrational quantum number
x	molar fraction.

Greek symbols

α	integrated band intensity
β	line-width to spacing parameter
γ	line-width
δ_k	vibrational transition number
$\Delta\varepsilon$	total emissivity overlap
ε_g	total gas emissivity
ν	wavenumber
ν_k	fundamental band k
τ_b	block transmissivity
ϕ	line-width-to-spacing temperature variation parameter
ψ	band-intensity temperature-variation parameter
ω	bandwidth parameter.

Subscripts

b	blackbody
c	band center (also designates CO_2)
i	gas species
j	band number
k	dummy variable
L	lower band limit
o	reference point
U	upper band limit
w	water vapor.

used in conjunction with the block approximation and band energy approximation. The calculation times using both methods are compared with the CPU time required by Smith and coworkers' sum of gray gases model (SGGM) [2], Leckner's [3] and Modak's [4] emissivity correlations and the modified box model of Steward and Kocaefe's [21].

2. EFFICIENT PROCEDURE FOR TOTAL RADIATIVE PROPERTY CALCULATIONS

2.1. *The exponential wide band model*

The exponential wide band model developed by Edwards and his co-workers [8–11] is based on a physical analysis of gas absorption. It provides a set of semi-empirical expressions to predict the total band absorptance of infrared active molecules. Presently, the EWBM can be used to predict the total radiative properties of any nitrogen-gas-soot mixtures including the following gases: H_2O, CO_2, CO, CH_4, NO, SO_2, N_2O, NH_3 and C_2H_2. The model can easily be adapted to incorporate other gases. It is believed that this model can be used to predict radiative properties in the temperature range $T \cong 300$ to 2500–3000 K, total pressure range $P_t \cong 0.5$–20 atm, volumetric fraction $x_i = 0$–1 and path length range $L \cong 10^{-4}$–100 m. It is generally accepted that the EWBM is about as accurate as the NBM for total emissivity and total band absorptance calculations, i.e. $\pm 20\%$. In addition, this model can easily be adapted to perform radiation calculations in non-homogeneous media.

Edwards and Menard [8] were the first to show that three physical parameters are necessary to describe total gas band absorptances over a wide range of temperature, path length and pressure conditions. These are:

the integrated band intensity $\alpha_{ij} \equiv \int_{\nu_{L,ij}}^{\nu_{U,ij}} \bar{k}_\nu \cdot d\nu$

the line-width-to spacing parameter $\beta_{ij} \equiv \pi\gamma/d \cdot Pe$,

and the bandwidth parameter ω_{ij}.

In the above relations, ν is the wavenumber [cm^{-1}], $\nu_{L,ij}$ and $\nu_{U,ij}$ are the lower and upper band limits of the jth band of species i, respectively. The parameter $\bar{k}_\nu$ is the mass absorption coefficient, γ and d are the average line width and average line spacing over a vibration-rotation band and P_e is the equivalent broadening pressure. Theoretically, the parameters α_{ij}, β_{ij} and ω_{ij} are functions of temperature, pressure and wave number. In the EWBM, it is assumed that the three parameters vary solely with temperature over each vibration–rotation band [10]. The influence of pressure upon the total band absorptance is accounted for through the pressure broadening parameter P_e, while the parameter $\bar{k}_\nu$ accounts for the spectral dependence. The derivation of analytical expressions for the temperature dependence of α_{ij}, β_{ij} and ω_{ij} has been given by Edwards and Menard [8], Weiner and Edwards [9] and Edwards and Balakrishnan [10]. A detailed presentation of the EWBM can be found in Edwards' monograph [11].

The bandwidth parameter $\omega_{ij}(T)$ is the width of the mean absorption coefficient $\bar{k}_v$ at 1/e of its maximum value. In the EWBM, the temperature dependence of $\omega_{ij}(T)$ is given by the simple expression $\omega_{ij}(T) = \omega_o \times \sqrt{T/T_o}$, where ω_o is the bandwidth parameter at the reference temperature T_o. Values for ω_o have been tabulated by Edwards and Balakrishnan [10] for the important infrared absorption bands of H_2O, CO_2, CH_4, CO, SO_2 and NO. A new database that incorporates corrections to the wide band parameters of H_2O [12] and CH_4 [16] as well as the three new species C_2H_2 [13], N_2O [14] and NH_3 [15] has recently been made available [6].

The *integrated band intensity* parameter α_{ij} represents the area under the curve $\bar{k}_v$. It is defined as

$$\alpha_{ij} = \int_0^\infty \bar{k}_v \cdot \mathrm{d}v. \tag{1}$$

In the EWBM, the functional dependence of α_{ij} with temperature is given by the relation [17]

$$\alpha_{ij}(T) = \alpha_o \frac{\left[1 - \exp\left(-\sum_{k=1}^{m} u_k \delta_k\right)\right] \cdot \psi(T)}{\left[1 - \exp\left(-\sum_{k=1}^{m} u_{o,k} \delta_k\right)\right] \cdot \psi(T_o)} \tag{2}$$

where

$$\begin{cases} u_k = C_2 \cdot \dfrac{v_k}{T} \quad \text{and} \quad u_{o,k} = C_2 \cdot \dfrac{v_k}{T_o} \\ v_k = 1/\lambda_k \quad \text{and} \quad T_o = 100\ K. \end{cases}$$

C_2 is Planck second radiation constant ($C_2 = 1.438786 \times 10^{-2}$ m·K) and $\psi(T)$ is defined as

$$\psi(T) \equiv \frac{\prod_{k=1}^{m} \sum_{v_k = v_{o,k}}^{\infty} \frac{(v_k + g_k + |\delta_k| - 1)!}{(g_k - 1)! v_k!} \mathrm{e}^{-u_k v_k}}{\prod_{k=1}^{m} \sum_{v_k = 0}^{\infty} \frac{(v_k + g_k - 1)!}{(g_k - 1)! v_k!} \mathrm{e}^{-u_k v_k}}. \tag{3}$$

In formulae (2), (3) and (6), v_k is the vibrational quantum number, g_k is the degeneracy of the fundamental band v_k and δ_k is the vibrational transition number. Values for α_o, g_k, δ_k and v_k can be found in Edwards' monograph [11] or in the more recent Table of ref. [6]. $v_{o,k}$ denotes the lowest possible initial state and is equal to zero when δ_k is positive or zero and otherwise to δ_k's absolute value. It should be noted that the algebraic sign is to be used with δ_k in the exponential term of equation (2), while the absolute value in equations (3) and (6).

2.2. *Optimized procedure for the calculation of* α_{ij}

Clearly, the computation of $\alpha_{ij}(T)$ and especially of the function $\psi(T)$ can slow down substantially the total radiative properties calculations if the series appearing in equation (3) is evaluated directly. In fact, it is possible to evaluate analytically the series appearing in the definition of $\psi(T)$. Weiner and Edwards [9] developed exact analytical expressions for the 6.3 and 2.7 μm bands of water vapor. Edwards [11] presented analytical expressions for the 15, 10.4 and 4.3 μm bands of carbon dioxide. Similar relations for the three infrared absorption bands of acetylene and nitrous oxide have also been given by Brosmer and Tien [13] and Tien *et al.* [14], respectively. To the authors' knowledge, no exact analytical expression for $\psi(T)$ has been published for other chemical species. This is quite surprising considering the potential of such expressions, both in simplifying and speeding up radiative properties calculations. For this reason, analytical expressions for $\psi(T)$ have been developed for all the infrared absorption bands of H_2O, CO_2, CH_4, CO, SO_2, NO, N_2O, NH_3 and C_2H_2. The expressions or the function $\psi(T)$, together with the integrated band intensity $\alpha_{ij}(T)$ are given in Table 1. The main advantage for using such simplified expressions is clear: the integrated intensity $\alpha_{ij}(T)$ of all the fundamental bands is constant, independent of temperature. Therefore, the integrated band intensity of about half of the absorption bands does not require any calculation.

2.3. *Optimized procedure for the calculation of* β_{ij}

In the exponential wide band model, the parameter β_{ij} is defined as π times the mean line-width to spacing ratio for a dilute mixture at one atmosphere total pressure, i.e.

$$\beta_{ij} \equiv \frac{\pi \cdot \gamma}{d \cdot Pe}. \tag{4}$$

Weiner and Edwards [9] derived the following relation for the functional dependence of β_{ij} with temperature:

$$\beta_{ij}(T) = \beta_o \left(\frac{T_o}{T}\right)^{1/2} \frac{\Phi(T)}{\Phi(T_o)} \tag{5}$$

where $\Phi(T)$ is defined as

$$\Phi(T) \equiv \frac{\left\{\prod_{k=1}^{m} \sum_{v_k = v_{o,k}}^{\infty} \left[\frac{(v_k + g_k + |\delta_k| - 1)!}{(g_k - 1)! v_k!} \mathrm{e}^{-u_k v_k}\right]^{1/2}\right\}^2}{\prod_{k=1}^{m} \sum_{v_k = v_{o,k}}^{\infty} \frac{(v_k + g_k + |\delta_k| - 1)!}{(g_k - 1)! v_k!} \mathrm{e}^{-u_k v_k}}. \tag{6}$$

Values for β_o can be found in refs. [6, 10, 11–16]. The denominator of equation (5) is identical to the numerator of relation (3), so that the calculation of $\Phi(T)$ is reduced to the evaluation of the infinite series appearing in the numerator of equation (6).

An approximate expression to the series appearing in $\Phi(T)$'s numerator was presented by Weiner and Edwards (see equation (28) of ref. [9]). However, no exact analytical expressions seem to exist. Therefore, the series in $\Phi(T)$'s numerator have to be evaluated numerically, which is often computationally expensive. Plots of $\beta_{ij}/\beta_o \times (T_o/T)^{-1/2}$ vs temperature are

Table 1. Simplified relations for the calculation of the integrated band intensity $\alpha(T)$

Bands (μm)	$\psi_{nom}(T)$[1]	$\psi(T)$	$\alpha(T)$ [cm^{-1}/g·m^{-2}]
		H_2O	
6.3	S_2^2[2]	S_2	α_o
2.7[3]	$2\cdot S_2^3$	$2\cdot S_2^2$	equation (2)
	S_1^2	S_1	α_o
	S_3^2	S_3	α_o
1.87	$(S_2\cdot S_3)^2$	$S_2\cdot S_3$	equation (2)
1.38	$(S_1\cdot S_3)^2$	$S_1\cdot S_3$	equation (2)
		CO_2	
15	$2\cdot S_2^3$	$2\cdot S_2$	α_o
10.4	$(S_1^2-1)\cdot S_3^2$	$e^{-u_1}(2-e^{-u_1})S_1\cdot S_3$	equation (2)
9.4	$(S_1^2-1)\cdot S_3^2$	$e^{-u_1}(2-e^{-u_1})S_1\cdot S_3$	equation (2)
4.3	S_3^2	S_3	α_o
2.7	$(S_1\cdot S_3)^2$	$S_1\cdot S_3$	equation (2)
2.0	$2\cdot S_1^3\cdot S_3^2$	$2\cdot S_1^2\cdot S_3$	equation (2)
		CO	
4.7	S_1^2	S_1	α_0
2.35	$2\cdot S_1^3$	$2\cdot S_1^2$	equation (2)
		NO	
5.34	S_1^2	S_1	α_o
		CH_4	
7.66	$6\cdot S_4^4$	$3\cdot S_4$	α_o
3.31	$6\cdot S_3^4$	$3\cdot S_3$	α_o
2.37	$6\cdot S_1^2\cdot S_4^4$	$3\cdot S_1\cdot S_4$	equation (2)
1.71	$24\cdot S_1^2\cdot S_2^3\cdot S_3^3\cdot S_4^4$	$6\cdot S_1\cdot S_2\cdot S_4$	equation (2)
		SO_2	
19.27	S_2^2	S_2	α_o
8.68	S_1^2	S_1	α_o
7.35	S_3^2	S_3	α_o
4.34	$2\cdot S_1^3$	$2\cdot S_1^2$	equation (2)
4.0	$(S_1\cdot S_3)^2$	$S_1\cdot S_3$	equation (2)
		NH_3	
10.5	S_2^2	S_2	α_o
6.15	S_4^2	S_4	α_o
3.0	S_1^2	S_1	α_o
		C_2H_2	
13.72	$2\cdot S_5^3$	S_5	α_o
7.53			ref. [13]
3.04	S_3^2	S_3	α_o
		N_2O	
7.8	S_1^2	S_1	α_o
4.5	S_3^2	S_3	α_o

[1] ψ_{nom} denotes the numerator of the function $\Psi(T)$ [see equation (3)]. It is also the denominator of equation (6).

[2] S_k is defined by the following equation:

$$S_k \equiv \frac{1}{1-e^{-u_k}} \quad \text{where} \quad u_k \equiv C_2\frac{\nu_k}{T}$$

[3] The 2.7 μm H_2O band consists of three overlapping bands. The overall integrated band intensity is obtained by summing the three bands contributions for this band, i.e.

$$\bar{\alpha}_{2.7} = \sum_{j=1}^{3}\alpha_{2.7,j}; \quad \beta \text{ is given by: } \bar{\beta}_{2.7} = \left\{\sum_{j=1}^{3}\left(\alpha_j\cdot\beta_j\right)\right\}\Big/\bar{\alpha}_{2.7}.$$

given in Figs. 1–6 for the absorption bands of H_2O, CO_2, CH_4, CO, NO and SO_2. These figures indicate that the dimensionless parameters $\beta_{ii}/\beta_o\times(T_o/T)^{-1/2} = \Phi(T)/\Phi(T_o)$ are simple monotonic functions of temperature. This suggests that the band parameters $\beta_{ii}(T)$ may be well approximated by expressions of the form

$$\beta_{ii}(T) \simeq \beta_o\cdot\sqrt{\frac{T_o}{T}}\cdot\left(\sum_{k=0}^{N}a_k\cdot T^k\right). \tag{7}$$

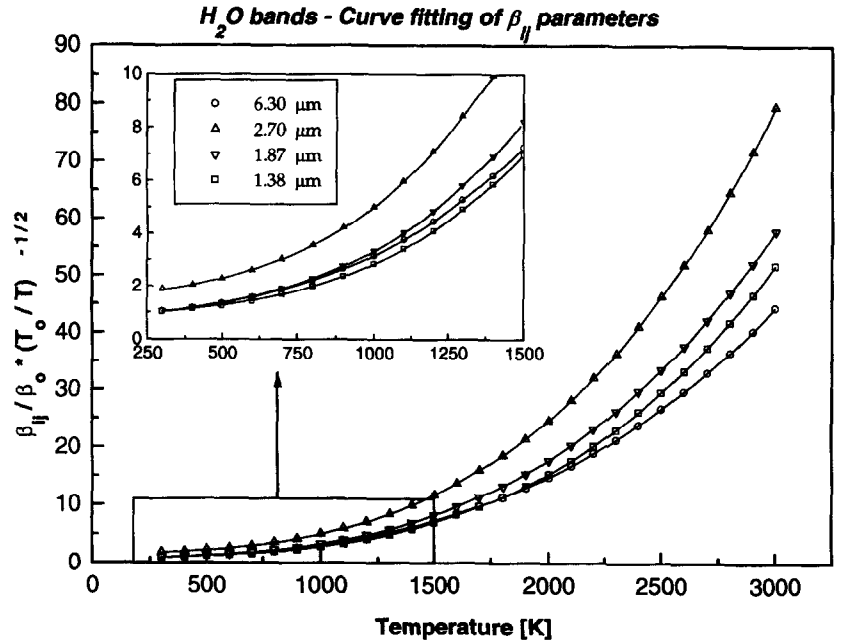

Fig. 1. Comparison between the predictions of the dimensionless group $\beta_{ij}/\beta_o \times (T_o/T)^{-1/2}$ using the exact equations (4) and (5) (symbols) and those obtained using the 'polynomial' approximation—equation (7) (solid lines)—for the 6.3, 2.7, 1.87 and 1.38 μm bands of water vapor.

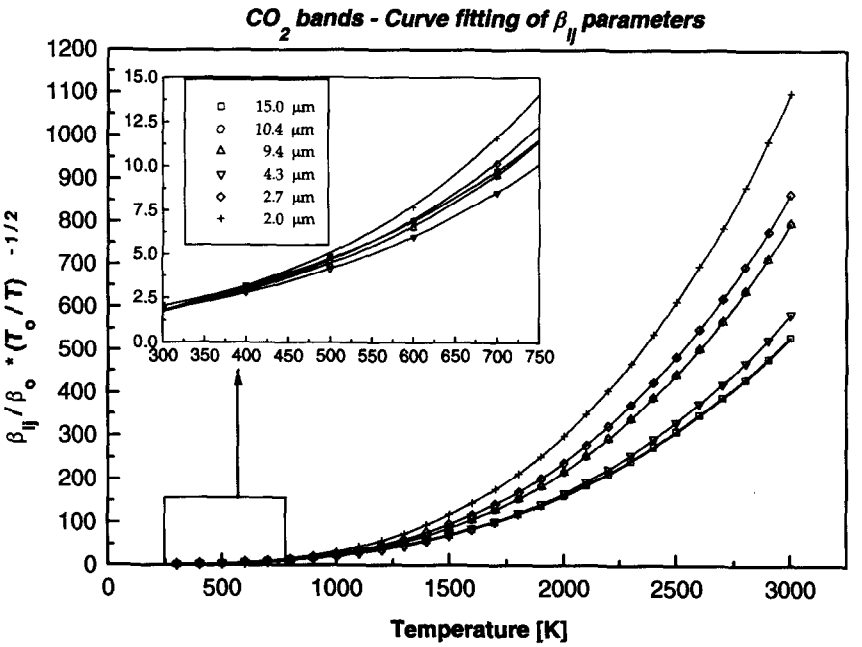

Fig. 2. Comparison between the predictions of the dimensionless group $\beta_{ij}/\beta_o \times (T_o/T)^{-1/2}$ using the exact equations (4) and (5) (symbols) and those obtained using the 'polynomial' approximation—equation (7) (solid lines)—for the 15, 10.4, 9.4, 4.3, 2.7 and 2.0 μm bands of carbon dioxide.

The band parameters $\beta_{ij}(T)$ have been calculated in the temperature range $300 \leqslant T \leqslant 3000$ K for the absorption bands of H_2O, CO_2, CH_4, CO, SO_2 and NO. The results of these calculations were used to fit a third-, fourth- and fifth-order polynomial using a general linear least square method. The choice of polynomials of degree four was found to provide the best compromise between the accuracy and generality requirements of the fit over the temperature range 300–3000 K. The fitting coefficients a_k are listed in Table 2 for the bands of the six chemical species considered. No correlation is given for either the 10 μm rotational band of water vapor or the bands of N_2O, NH_3 and C_2H_2 since the relationships to calculate the

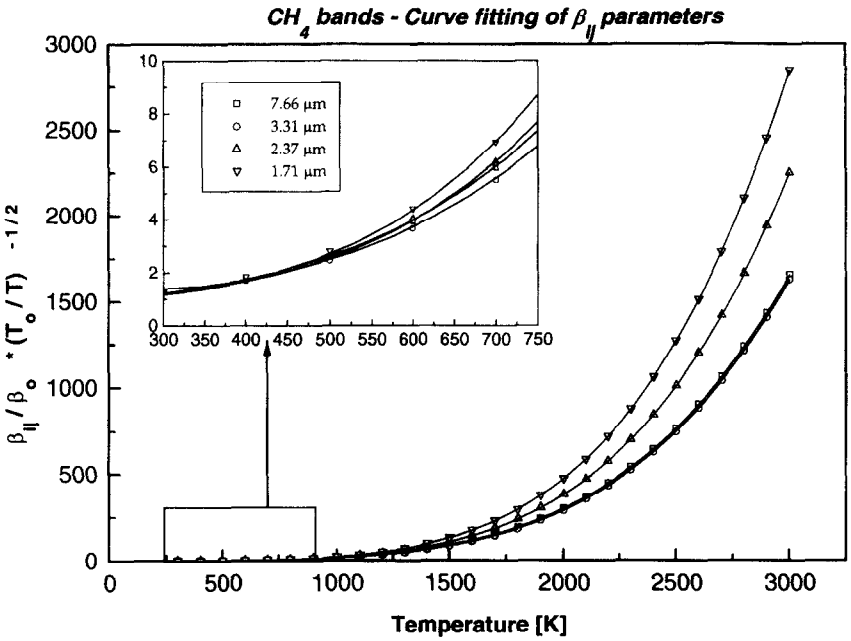

Fig. 3. Comparison between the predictions of the dimensionless group $\beta_{ij}/\beta_o \times (T_o/T)^{1/2}$ using the exact equations (4) and (5) (symbols) and those obtained using the 'polynomial' approximation—equation (7) (solid lines)—for the 7.66, 3.31, 2.37 and 1.71 μm bands of methane.

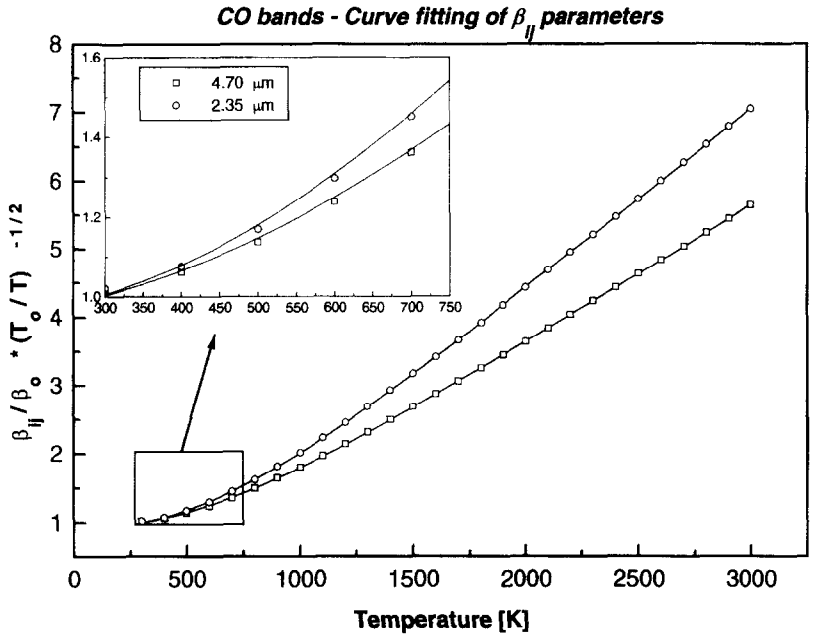

Fig. 4. Comparison between the predictions of the dimensionless group $\beta_{ij}/\beta_o \times (T_o/T)^{1/2}$ using the exact equations (4) and (5) (symbols) and those obtained using the 'polynomial' approximation—equation (7) (solid lines)—for the 4.7 and 2.35 μm bands of carbon monoxide.

β_{ij}s of these gases are already given in the form of simple analytical expressions [6, 11–16].

The average and maximum absolute errors between the equation (7) predictions and the numerical evaluation of equations (5) and (6) are listed in Table 3. For temperatures above 800 K, relation (7) yields β_{ij} predictions to within 1% of the exact numerical results obtained using equations (5) and (6). For H_2O, CO, SO_2 and NO, the maximum absolute errors never exceed 2%. Though larger, the maximum absolute errors recorded for CO_2 and CH_4 are in most cases well below 10%. It was observed that the relative error decreases rapidly with increasing temperature [6]. For instance, at 300 K, the maximum deviation for the

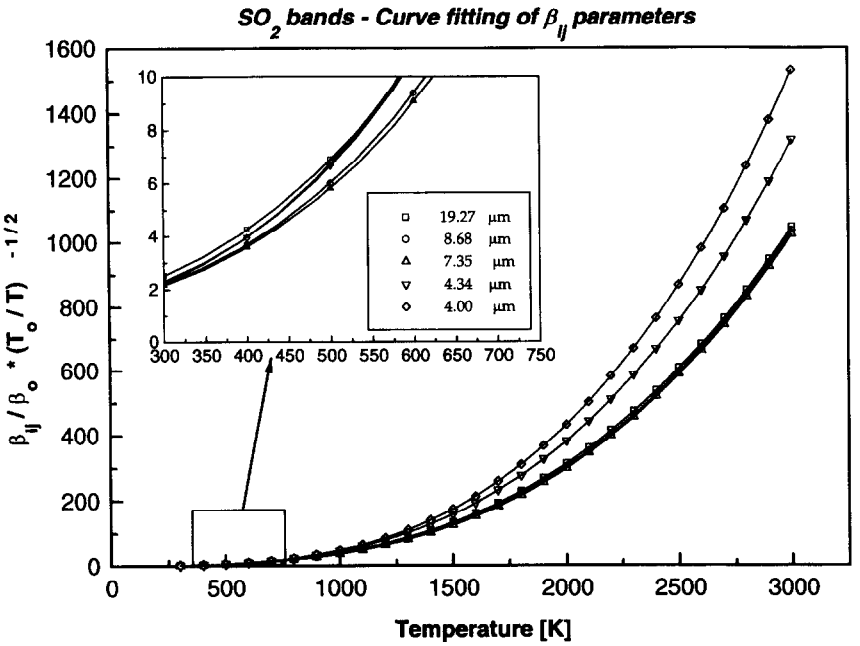

Fig. 5. Comparison between the predictions of the dimensionless group $\beta_{ij}/\beta_o \times (T_o/T)^{-1/2}$ using the exact equations (4) and (5) (symbols) and those obtained using the 'polynomial' approximation—equation (7) (solid lines)—for the 19.27, 8.68, 7.35, 4.34 and 4.0 μm bands of sulfur dioxide.

Table 2. Fitting coefficients for the calculation of the line-width to spacing ratio parameter $\beta_{ij}(T)$ of H_2O, CO_2, CH_4, CO, SO_2 and NO in the temperature range 300–3000 K [see equation (7)]

Bands [m]	a_0	a_1	a_2	a_3	a_4
			H_2O		
6.3	0.842307	3.79754×10^{-4}	6.68034×10^{-7}	1.23242×10^{-9}	3.9887×10^{-14}
2.7	1.540955	7.48362×10^{-4}	3.48073×10^{-7}	2.21254×10^{-9}	1.5899×10^{-13}
1.87	0.744548	9.02501×10^{-4}	-2.69531×10^{-7}	1.88458×10^{-9}	7.4664×10^{-14}
1.38	0.795496	7.58821×10^{-4}	-4.69848×10^{-7}	1.65543×10^{-9}	1.0327×10^{-13}
			CO_2		
15	0.196135	4.60263×10^{-3}	-6.54262×10^{-7}	1.93769×10^{-8}	4.6826×10^{-15}
10.4	−1.656057	1.49517×10^{-2}	-2.22210×10^{-5}	3.34193×10^{-8}	6.3939×10^{-13}
9.4	−1.642894	1.48960×10^{-2}	-2.21505×10^{-5}	3.33859×10^{-8}	6.4455×10^{-13}
4.3	−0.465200	8.65064×10^{-3}	-1.09215×10^{-5}	2.41811×10^{-8}	6.1291×10^{-14}
2.7	−1.563141	1.49529×10^{-2}	-2.40186×10^{-5}	3.80780×10^{-8}	1.4219×10^{-13}
2.0	−2.333098	1.96932×10^{-2}	-3.48132×10^{-5}	5.02315×10^{-8}	7.2356×10^{-15}
			CH_4		
7.66	1.564842	-6.894421×10^{-3}	2.54499×10^{-5}	-2.84493×10^{-8}	2.7312×10^{-11}
3.31	1.433591	-6.750206×10^{-3}	2.66633×10^{-5}	-3.18397×10^{-8}	2.7962×10^{-11}
2.37	4.523660	-2.470598×10^{-2}	6.36154×10^{-5}	-6.60821×10^{-8}	4.3582×10^{-11}
1.71	5.269932	-3.061382×10^{-2}	8.01309×10^{-5}	-8.63644×10^{-8}	5.6101×10^{-11}
			CO		
4.70	0.968458	-3.19407×10^{-4}	1.58693×10^{-6}	-4.95428×10^{-10}	5.8419×10^{-14}
2.35	0.989397	-5.32794×10^{-4}	2.13906×10^{-6}	-6.57943×10^{-10}	7.6326×10^{-14}
			SO_2		
19.27	0.358415	4.26431×10^{-3}	-1.85430×10^{-6}	3.89339×10^{-8}	-5.7857×10^{-15}
8.68	0.234585	5.13241×10^{-3}	-7.29580×10^{-6}	4.03494×10^{-8}	-5.6772×10^{-14}
7.35	0.124110	5.94186×10^{-3}	-9.34916×10^{-6}	4.05602×10^{-8}	-6.9248×10^{-14}
4.34	0.334783	5.54569×10^{-3}	-1.23091×10^{-5}	5.30622×10^{-8}	-2.7098×10^{-13}
4.00	−0.795474	1.25562×10^{-2}	-2.76297×10^{-5}	6.52692×10^{-8}	-2.2545×10^{-13}
			NO		
5.34	0.896005	-6.34331×10^{-5}	1.67418×10^{-6}	-5.3493×10^{-10}	6.4022×10^{-14}

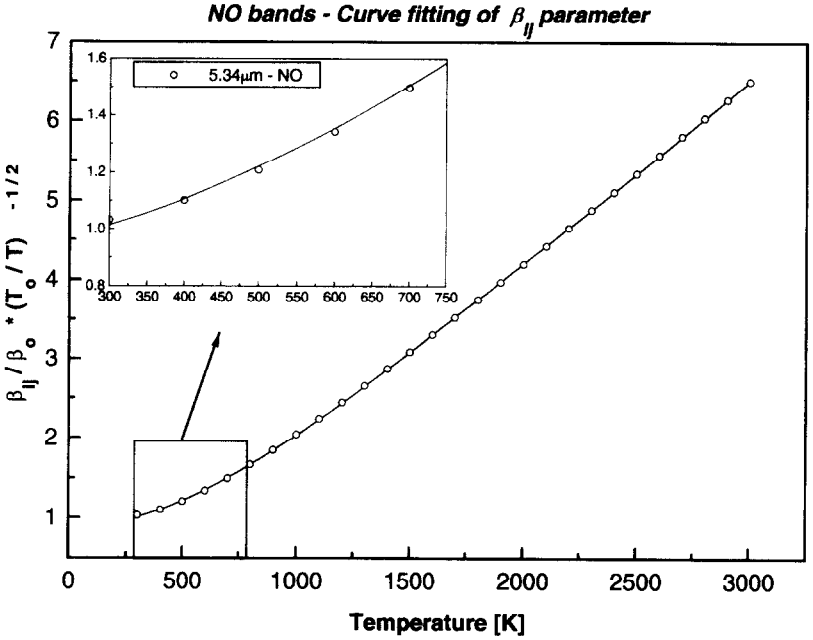

Fig. 6. Comparison between the predictions of the dimensionless group $\beta_{ij}/\beta_o \times (T_o/T)^{1/2}$ using the exact equations (4) and (5) (symbols) and those obtained using the 'polynomial' approximation—equation (7) (solid lines)—for the 5.34 μm band of nitrogen oxide.

2.37 μm band of CH_4 is about 10%. This deviation decreases to less than 0.5% at 800 K and 0.002% at 2500 K [6].

3. ERROR INTRODUCED BY THE USE OF EQUATION (7) IN TOTAL EMISSIVITY CALCULATIONS

It may be questioned how the errors introduced by the use of equation (7) reflect on the accuracy of the total emissivity calculations. An estimate of this effect is performed for gas mixtures involving the contribution of only one absorbing gas. The total emissivities of gas mixtures including H_2O–N_2, CO_2–N_2, CO–N_2, NO–N_2, SO_2–N_2 and CH_4–N_2 are calculated in the temperature range 300–3000 K, path length range 10^{-4}–100 m and molar fractions x_i of the absorbing gas 'i' equal to 0.1, 0.5 and 1.0. The maximum absolute error between the predictions obtained using either equations (5) and (6) or equation (7) are shown in Table 4. The total emissivity predictions using equation (7) are, with one exception, all within 1% of the exact results. As shown in Table 4, maximum errors of about 2% appear for CH_4–N_2 mixtures at a 10 cm path length. The maximum errors are observed, as in the case of the β_{ij} parameters, at a temperature of 300 K.

4. SPEED TESTS RESULTS

In order to quantify the reduction in CPU time which results from the simplifications, two tests have been carried out. In the first test, the total emissivities of five different gas mixtures are computed using the 'block approximation' (BA) proposed by Edwards [11]. In the second test, the so called 'band energy approximation' (BEA) is used.

In the block approximation, the total emissivity of a gas mixture having N distinct spectral regions is given by

$$\varepsilon_g \cong \sum_{k=1}^{N} (1 - \bar{\tau}_{b,k}) \left[f\left(\frac{\nu_{bL,k}}{T}\right) - f\left(\frac{\nu_{bU,k}}{T}\right) \right]. \quad (8)$$

In the above relation, $\bar{\tau}_{b,k}$ is the spectral block transmissivity, $\nu_{bL,k}$ and $\nu_{bU,k}$ are the lower and upper wavenumber limits of block k, respectively, T is the gas temperature and $f(x)$ is the fractional function of blackbody radiation. In this method, the band transmissivity is assumed constant over the whole band width, which is a valid assumption only when the bands are completely saturated and/or when the spectral intervals are small. In the first test, the CPU time required to calculate the total emissivity using equations (2), (3), (5), (6) on the one hand and equation (8) on the other are recorded for four different gas mixtures. The results are listed in Table 5 as method 1. The series in equations (3) and (6) are calculated until an accuracy of 10^{-8} is reached. The computational runs (method 2 in Table 5) are repeated with equation (3) replaced by the analytical expressions listed in Table 1, and equations (5) and (6) replaced by equation (7). Typical run times for the total emissivity calculations of mixtures of one, two, three and four chemical species using both methods are presented in Table 5. The advantage of using the analytical expressions listed in Table 1 to calculate $\alpha_{ij}(T)$ and relation (7) is clearly demonstrated.

Table 3. Comparison between the exact calculations of the β_{ij} parameter using equations (5) and (6) and the predicted values given by equation (7) in the temperature range $300 \leqslant T \leqslant 3000$ K

Chemical species and related absorption bands	Average absolute error [%]	Maximum absolute error [%]	Temperature above which the absolute error is always less than 1%
	H_2O		
6.3 μm	0.19	1.42	800 K
2.7 μm	0.15	1.23	400 K
1.87 μm	0.21	1.86	600 K
1.38 μm	0.23	1.82	600 K
	CO_2		
15 μm	0.05	0.77	300 K
10.4 μm	0.57	8.30	700 K
9.4 μm	0.56	8.20	700 K
4.3 μm	0.23	3.30	600 K
2.7 μm	0.47	6.82	700 K
2.0 μm	0.57	8.65	700 K
	CH_4		
7.66 μm	0.27	3.23	400 K
3.31 μm	0.51	6.27	800 K
2.37 μm	0.77	9.65	700 K
1.71 μm	0.78	9.00	700 K
	SO_2		
19.27 μm	0.03	0.37	300 K
8.68 μm	0.05	0.65	300 K
7.35 μm	0.06	0.86	300 K
4.34 μm	0.05	0.63	300 K
4 μm	0.13	2.00	300 K
	CO		
4.7 μm	0.26	1.40	400 K
2.35 μm	0.26	1.50	400 K
	NO		
5.34 μm	0.29	1.77	600 K

Equation (8) further necessitates the computation of the fractional blackbody function $f(v/T)$. The latter is easily evaluated using the appropriate series expansion [18]. The time required to compute $f(v/T)$ is often comparable to the time required to calculate the block's transmissivity $\bar{\tau}_{b,k}$. The analysis of the series given in ref. [18] reveals that little can be done to further optimize the computation of the function $f(v/T)$. On the other hand, it is possible to avoid computing $f(v/T)$ if the 'band energy approximation' is invoked to calculate total radiative properties [11].

The BEA assumes that the blackbody emissive power is constant over each absorption band. This method is likely to be inaccurate in gas mixtures having wide emission/absorption bands, since the blackbody emissive power may vary substantially over the width of the band. The BEA is thus more likely to be inaccurate at high pressures. This effect is even stronger for bands located near the maximum spectral blackbody emissive power. Furthermore, it is not well adapted for gas mixtures having numerous overlapping bands, since the treatment of overlapping regions often requires special mathematical procedures. Although calculations of both emissivity and total band absorptance of gases having overlapping spectral bands have been the subject of many research studies [12, 19, 20], no general and simple methods exist to account for bands overlapping using the BEA. To date, all the remedies which have been proposed to tackle this problem clearly lack generality [12, 19, 20]. The application of methods such as those presented in refs. [19, 20] is possible, provided knowledge of the relative strength of the overlapping bands is available.

In view of the lack of comparative tests, the BEA is not recommended for gas mixtures containing more than two absorbing gases having common overlapping bands. However, the simplicity of the band energy approximation formulation makes it often the preferred method to compute H_2O–CO_2 total emissivity [4, 13, 16]. In the BEA, the total emissivity of H_2O–CO_2 mixtures is expressed as

$$\varepsilon_g \cong \sum_{k=1}^{N} \frac{\bar{E}^{o}_{v_{C,k}}}{\sigma \cdot T^4} \cdot A_k - \Delta\varepsilon_{c+w} \tag{9}$$

where $\bar{E}^{o}_{v_{C,k}}(T)$ is the blackbody emissive power cal-

Table 4. Approximate model maximum relative errors (%) for the calculation of the total emissivity of H_2O–N_2, CO_2–N_2, CH_4–N_2, CO–N_2, SO_2–N_2 and NO–N_2 gas mixtures in the temperature range 300–3000 K and pathlength range $Le = 10^{-4}$–100 m

	$x_i = 0.1$	$x_i = 0.5$	$x_i = 1$
	H_2O		
$Le = 10^{-4}$ m	0	0	0
$Le = 10^{-2}$ m	0.08	0.10	0.14
$Le = 1$ m	0.12	0.06	0.05
$Le = 100$ m	0.06	0.05	0.04
	CO_2		
$Le = 10^{-4}$ m	0	0.07	0.22
$Le = 10^{-2}$ m	0.37	0.37	0.32
$Le = 1$ m	0.17	0.12	0.12
$Le = 100$ m	0.28	0.51	0.59
	CH_4		
$Le = 10^{-4}$ m	0	0	0
$Le = 10^{-2}$ m	1.28	1.49	1.54
$Le = 1$ m	1.00	0.65	0.56
$Le = 100$ m	0.42	0.35	0.33
	CO		
$Le = 10^{-4}$ m	0	0	0.09
$Le = 10^{-2}$ m	0.59	0.66	0.67
$Le = 1$ m	0.49	0.32	0.28
$Le = 100$ m	0.20	0.17	0.17
	NO		
$Le = 10^{-4}$ m	0	0	0
$Le = 10^{-2}$ m	0.53	0.76	0.80
$Le = 1$ m	0.52	0.35	0.31
$Le = 100$ m	0.22	0.19	0.18
	SO_2		
$Le = 10^{-4}$ m	0	0	0
$Le = 10^{-2}$ m	0.13	0.15	0.16
$Le = 1$ m	0.15	0.09	0.07
$Le = 100$ m	0.05	0.04	0.04

culated at the band centre $\nu_{C,k} \equiv (\nu_{L,k} + \nu_{U,k})/2$ and A_k is the total band absorptance of the band $[\nu_{L,k} - \nu_{U,k}]$. The correction $\Delta\varepsilon_{c+w}$ accounts for the overlapping of the 2.7 and 15 μm bands. The simplified procedure proposed by Modak (see equations (D1) and (D2) of ref. [12]) is used in the present study to calculate $\Delta\varepsilon_{c+w}$. The CPU time required to calculate the total emissivity of H_2O–N_2, CO_2–N_2 and H_2O–CO_2–N_2 mixtures using the analytical expressions listed in Table 1 for $\alpha_{ij}(T)$, relation (7) for $\beta_{ij}(T)$, and the band energy approximation were recorded and are compared with the time necessary to calculate the total emissivity using the block approximation (see rows two to four of Table 6).

Run time estimates required to calculate the total emissivity of mixtures of three and four absorbing gases are also listed in Table 6. The calculations are performed assuming the CO and CH_4 bands do not overlap with the CO_2 and H_2O bands. It is believed that these times are very good estimates of the computational time required if overlapping has been taken into account. Indeed, the time necessary to compute band overlapping using a correlation such as that of ref. [19] is only a small fraction of the overall CPU time required to calculate the total emissivity of H_2O–CO_2 gas-mixture. Furthermore, as pointed out by one of the reviewers of this article, the contribution of CO and CH_4 is likely to be small in most fossil fuel combustion problems, so that neglect of the overlapping should only have a small impact on the total heat transfer calculations. This effect will be even more prominent in luminous flames.

It is clear that the BEA method is computationally more attractive than the BA method for implementation in CFD computer codes. In most cases, the maximum discrepancy between emissivity cal-

Table 5. Computing time (in milliseconds) required (PC 386 running at 25 MHz with a 80387 processor) to calculate the total emissivity of various gas mixtures using the EWBM. Method 1 uses equations (2) (3) (5) and (6) to compute the parameters α_{ij} and β_{ij}. Method 2 uses equations (2) and (7), Table 1 and Table 2

Gas mixtures	Method 1	Method 2	Acceleration factor between method 2 and 1
H_2O[(1)]	163	5.8	28
CO_2[(2)]	587	6.0	98
H_2O, CO_2[(3)]	750	12.8	59
H_2O, CO_2, CO[(4)]	777	16.6	47
H_2O, CO_2, CO, CH_4[(5)]	1033	23.1	45

[(1)] $P_T = 1$ atm, $T = 1500$ K, $L = 0.01$ m, $x_{H_2O} = 0.16$.
[(2)] $P_T = 1$ atm, $T = 1500$ K, $L = 0.01$ m, $x_{CO_2} = 0.09$.
[(3)] $P_T = 1$ atm, $T = 1500$ K, $L = 0.01$ m, $x_{H_2O} = 0.16$, $x_{CO_2} = 0.09$.
[(4)] $P_T = 1$ atm, $T = 1500$ K, $L = 0.01$ m, $x_{H_2O} = 0.16$, $x_{CO_2} = 0.09$, $x_{CO} = 0.02$.
[(5)] $P_T = 1$ atm, $T = 1500$ K, $L = 0.01$ m, $x_{H_2O} = 0.16$, $x_{CO_2} = 0.09$, $x_{CO} = 0.02$, $x_{CH_4} = 0.01$.

Table 6. Comparison of the CPU time required to calculate the total emissivity of various gas mixtures using the block approximation (BA) and the band energy approximation (BEA). The gas mixtures are the same as those listed in Table 5. All the times are in milliseconds. Values in parentheses are the predicted total emissivities

Gas mixtures	(BA) See equation (8)	(BEA) See equation (9)	Ratio
H_2O	5.8	2.6	2.2
	(0.0034)	(0.0031)	
CO_2	6.0	2.5	2.4
	(0.0075)	(0.0077)	
H_2O, CO_2	12.8	5	2.6
	(0.0109)	(0.0109)	
H_2O, CO_2, CO	16.6	5.6	3.0
	(0.0110)	(0.0110)	
H_2O, CO_2, CO, CH_4	23.1	7	3.3
	(0.0112)	(0.0113)	

Table 7. Computing time (in milliseconds) required to calculate the total emissivity of three different gas mixtures. Values in parentheses are the predicted total emissivities

Gas mixtures	EWBM (BA)	EWBM (BEA)	Leckner [3]	Modak [4]	Steward and Kocaefe [21]	Smith *et al.* [2]
$H_2O^{(1)}$	5.9	2.8	0.6	2.1	2.7	—
	(0.185)	(0.185)	(0.170)	(0.168)	(0.151)	
$CO_2^{(2)}$	6.9	2.6	0.8	2.1	1.7	—
	(0.088)	(0.089)	(0.091)	(0.086)	(0.092)	
H_2O–$CO_2^{(3)}$	13.9	5.5	1.5	4.2	4.4	0.310
	(0.251)	(0.253)	(0.236)	(0.275)	(0.225)	(0.267)

(1) $P_T = 1$ atm, $T = 1500$ K, $L = 1$ m, $x_{H_2O} = 0.2$.
(2) $P_T = 1$ atm, $T = 1500$ K, $L = 1$ m, $x_{CO_2} = 0.1$.
(3) $P_T = 1$ atm, $T = 1500$ K, $L = 1$ m, $x_{H_2O} = 0.2$, $x_{CO_2} = 0.1$.

culations using the two methods is insignificant. However, it should be emphasized that the overlap emissivity correction is not always accurately predicted using the BEA. Therefore, it is only recommended for H_2O–CO_2 emissivity calculations at atmospheric pressure using the BA method for other situations.

5. RUNTIME COMPARISON BETWEEN THE EWBM AND VARIOUS H_2O–CO_2 EMISSIVITY CORRELATIONS

A comparison of the CPU time required for the EWBM calculations with that of some widely applied total emissivity correlations is important information for mathematical modelers. Therefore, additional tests were carried out to compare the EWBM's execution times to calculate the total emissivity of H_2O–N_2, CO_2–N_2 and an H_2O–CO_2–N_2 mixtures with the ones required by the emissivity correlations of Smith and coworkers [2], Leckner [3], Modak [4] and Steward and Kocaefe [21]. All the computer subroutines were optimized before testing.

It is clear from the results shown in Table 7 that the computing time required by the EWBM is, in the case of the band energy approximation (BEA), comparable to the CPU time required by the polynomial approximations (Leckner [3] and Modak [4]) and hybrid emissivity model [21]. For H_2O–CO_2–N_2 mixtures, Smith *et al.*'s [2] sum of gray gases model is about 15 times faster than the BEA method and 45 times faster than the block approximation method. Though computationally attractive, Smith *et al.*'s model [2] also has a number of shortcomings. It is limited to emissivity calculations at a total pressure of one atmosphere, H_2O to CO_2 partial pressure ratios equal to 1 and 2 and cannot easily be adapted to the emissivity calculations of mixtures of more than two gases having common overlapping bands. This makes these models less attractive for implementation in CFD computer codes for flame modeling.

The block approximations, though two to ten times slower than the other models tested, still appear competitive. On a computational grid with 20,000 cells, the use of the EWBM's block and energy band approximations would require 275 and 110 s, respectively, to calculate the total emissivity of H_2O–CO_2 mixtures of each grid node with a PC 386 running at 25 MHz and having a numerical processor. On a SUN-SPARC station 10, it is estimated that the same calculation would be run 10–20 times faster, i.e. would take between 5.5 and 24 s. For comparison, Leckner's polynomial approximations would take about 2 s to complete the same calculation on a SUN-SPARC10, while Modak's model would require approximately three times as much.

6. THE COUPLING OF EXISTING SOLUTION METHODS OF THE RADIATIVE TRANSFER EQUATION WITH THE EWBM

As with the statistical narrow band model (SNBM), the EWBM is based on the Goody absorption law [22]. Algorithms to perform radiation calculations in non-gray non-homogeneous media have been developed for both models. The basic idea in treating non-homogeneous problems is to replace the band parameters appearing in the Goody law by scaled quantities so that the homogeneous formulation remains valid in non-homogeneous situations. In the SNBM, the scaled parameters are determined by equating the isothermal and non-isothermal band transmittance in the weak and strong absorption limits [23]. A similar approach is used to find the wide band scaling parameters $\alpha_{ij,\mathrm{nh}}$, $\eta_{ij,\mathrm{nh}} = \beta_{ij} \cdot Pe$ and $\omega_{ij,\mathrm{nh}}$ appearing in the EWBM formulation [24, 25]. These common features of the EWBM and SNBM considerably restrict the choice of solution methods of the RTE with which these models and related scaling methods can be solved. Indeed, since both models focus on the prediction of the band transmissivity, a rigorous treatment of non-gray homogeneous and non-gray non-homogeneous radiation problems is theoretically possible using integral solution methods of the RTE.

6.1. *Integral solution methods of the RTE*

The main shortcoming of the EWBM in treating radiation problems in confined environments is that it does not easily account for the wall interactions. This problem originates from the nature of the EWBM which requires calculation of the total band absorptance prior to that of the band transmissivity and band width. Since the width of each absorption band varies with temperature, pressure and path-length, a different division of the infrared spectrum is required for each path along which the equation of radiative transfer is solved. Yet, to properly account for gas–walls interactions, it is necessary to use the same spectral division for the wall and for the gas properties. The implication of having a different spectrum along each radiation path yields to the conclusion that the spectral wall properties can only be set up once the equation of radiative transfer has been solved along each path within the gas volume (assuming no wall interactions). Ultimately, it may be inferred that this calculation procedure would require a larger amount of memory than the narrow band model itself, while being altogether more computationally expensive. Some of the main impediments to coupling the EWBM to the classical RTE solution methods have been further discussed by Edwards [32].

6.2. *Flux solution methods*

Kim *et al.* [26] recently attempted to couple the EWBM into the discrete ordinate solution method of the RTE. However, their approach to solve the discrete ordinate equations involves rewriting the latter into an integral form so that the EWBM algorithm can be used.

To date, the most promising approach to use the EWBM with flux solution methods is perhaps the spectral group model† (SGM) of Song and Viskanta [27, 28]. The EWBM is used to compute the gray gases coefficient appearing in the sum of gray gases formulation of the RTE. Although numerous sum of gray gases models exist, they are all limited to the partial pressure ratio of one and two, which, as shown in a recent paper [30] is not general enough to accommodate the variation of partial pressure existing in non-luminous swirling flames. The advantage of the Song and Viskanta Model [27] is that, in averaging the RTE over a fixed spectral interval, the spectrally averaged equation basically retains the same mathematical form as the original equation: thus enabling minor modifications to existing radiation solvers. Beyond pure combustion applications, the use of the EWBM based SGGM enables one to cover a wide range of heat transfer applications, including high pressure systems and high temperature chemical processes involving any mixture of H_2O, CO_2, CO, CH_4, NH_3, SO_2 and N_2. A major improvement of the EWBM based SGGM over classical SGGM is that the location and width of the bands are known *a-priori* so that an account of the wall non-grayness is theoretically possible. As reported recently by Song [28], for the one-dimensional radiation problem of Kim *et al.* [26], the computing time necessary to evaluate the SGM coefficients on a CRAY-2S is about 60 times greater than that required for calculating the heat fluxes using these coefficients. It is believed that the optimized procedure presented in this paper will help reduce the latter computational times. It should be emphasized that the use of the spectral group model along with coefficients of classical SGGM is not always accurate when dealing with gray walls that are hot and diffusively reflective [31].

6.3. *Applications*

The advantage of using the EWBM over both sum of gray gases models and SNBM is in applications involving gas mixtures for which narrow band model parameters have not yet been developed, namely SO_2, NH_3 and C_2H_2. The EWBM based sum of gray gases model of Song and Viskanta [27] offers further advantages if compared to classical SGGM [1, 2], in that it may be used to determine SGGM coefficients that are otherwise not yet available, such as in applications

† The authors of refs. [27, 28] employ the term spectral group model to describe a variant of the sum of gray gases model. Hereinafter, the term spectral group model is used to describe the solution method of the RTE, rather than the property model itself, since basically both existing SGGM and the radiative property model of Song and Viskanta [27] may be recast in a somewhat more general frame, namely that of the correlated-k distribution method [29].

including high pressure systems and high temperature chemical processes involving mixture of H_2O, CO_2, CH_4, CO, SO_2, NO, C_2H_2, N_2O and NH_3. The main application area of the EWBM along with the integrated form of the RTE is in systems for which wall interaction is small or non-existent. This includes fires and confined flames in cool furnaces. The integral formulation of the EWBM is also advantageous in applications involving turbulence radiation interactions [33]. Considering the EWBM is a general and accurate radiative property model and requires execution times which are about the same order of magnitude as more approximate models, it is recommended for implementation in CFD codes performing extensive radiative heat transfer calculations.

7. CONCLUSIONS

Exact analytical expressions for the integrated band intensity have been derived for the bands of H_2O, CO_2, CH_4, CO, SO_2, NO, C_2H_2, N_2O and NH_3. The calculations of the β_{ij} parameters have been substantially optimized by approximating the series expansion appearing in equation (5) and (6) by the polynomial correlation of equation (7). Use of this correlation provides 1% accuracy of total emissivity calculations if compared to exact (numerical) calculations. Both improvements are recommended for optimizing calculation using the exponential wide band model (EWBM).

The computational times required to calculate the total emissivity of various gas mixtures using this procedure bring the EWBM to within execution times comparable to that required for polynomial approximations [3, 4] or hybrid models [21]. Although the CPU times required by the block approximation (BA) method to calculate total gas emissivities are somewhat longer than those of the band energy approximation (BEA), it is believed that the former method is more reliable at elevated pressures and generally for gas mixtures having more than two absorbing species. The BEA is recommended for calculations at atmospheric pressure of a single absorbing gas. It can be used for H_2O–CO_2 emissivity calculations, provided the band overlapping in the 2.7 and 15 μm regions is accounted for using appropriate models [12, 19, 20]. Extensions of the BEA to other gas mixtures and high pressures, though possible, still require a detailed study comparing the overlap emissivity predictions with measured data.

The simplifications introduced into the calculations of the line-width-to-spacing parameter do not weaken the generality, nor substantially decrease the accuracy of the EWBM, while drastically reducing the computing time. The proposed simplifications to the EWBM make it an ideal property model for incorporating into CFD codes for flame calculations.

The coupling of the EWBM with the classical solution methods of the radiative transfer equation has been discussed. Radiative heat transfer calculations in open or confined environments for which the walls are cold and non-reflective may be handled using the integral form of the RTE along with appropriate wide band scaling relations [24, 25]. The spectral group formulation of the RTE along with sum of gray gases coefficients or EWBM based SGGM may also be used. However, it is not yet apparent how diffusively reflecting walls may be accurately handled using either methods.

Acknowledgements—This work was supported by the IFRF, the Institut Français du Pétrole (IFP), Electricity of France (EdF) and Gaz de France (GdF). The authors would like to thank A. Sayre for proof reading this manuscript as well as the reviewers for their critical reading of the documents and their constructive suggestions.

REFERENCES

1. P. B. Taylor and P. J. Foster, The total emissivities of luminous and non-luminous flames, *Int. J. Heat Mass Transfer* **17**, 1591–1605 (1974).
2. T. F. Smith, Z. F. Shen and J. N. Friedman, Evaluation of coefficients for the weighted sum of gray gases model, *ASME J. Heat Transfer* **104**, 602–608 (1982).
3. B. Leckner, Spectral and total emissivity of water vapor and carbon dioxide, *Combust. Flame* **19**, 33–48 (1972).
4. A. T. Modak, Radiation from products of combustion, *Fire Res.* **1**, 339–361 (1979).
5. A. A. F. Peters and R. Weber, Modeling of swirling natural gas and pulverised coal flames with emphasis on nitrogen oxides, IFRF Document no. F 36/y/21D (1993).
6. N. Lallemant and R. Weber, Radiative properties models for computing non-sooty natural gas flames, IFRF Document no. G08/y/2 (1994).
7. C. B. Ludwig, W. Malkmus, J. E. Reardon and J. A. L. Thomson, *Handbook of Infrared Radiation by Combustion Gases* (Edited by R. Goulard and J. A. L. Thomson), NASA SP-3080 (1973).
8. D. K. Edwards and W. A. Menard, Comparison of models for correlation of total band absorption, *J. Appl. Opt.* **3**, 621–625 (1964).
9. M. M. Weiner and D. K. Edwards, Theoretical expression of water vapor spectral emissivity with allowance for line structure, *Int. J. Heat Mass Transfer* **11**, 55–65 (1968).
10. D. K. Edwards and A. Balakrishnan, Thermal radiation by combustion gases, *Int. J. Heat Transfer* **16**, 25–40 (1973).
11. D. K. Edwards, Molecular gas band radiation. In *Advances in Heat Transfer* (Edited by T. F. Irvine, Jr and J. P. Harnett), Vol. 12, pp. 115–193. Academic Press, New York (1976).
12. A. T. Modak, Exponential wide band parameters for the pure rotational band of water vapor, *J. Quant. Spectrosc. Radiat. Transfer* **21**, 131–142 (1979).
13. M. A. Brosmer and C. L. Tien, Thermal radiation properties of acetylene, *ASME J. Heat Transfer* **107**, 943–948 (1985).
14. C. L. Tien, M. F. Modest, C. R. McCreight, Infrared radiation properties of nitrous oxide, *J. Quant. Spectrosc. Radiat. Transfer* **12**, 267–277 (1972).
15. C. L. Tien, Band and total emissivity of ammonia, *Int. J. Heat Mass Transfer* **16**, 856–857 (1973).
16. M. A. Brosmer and C. L. Tien, Infrared radiation properties of methane at elevated temperature, *J. Quant. Spectrosc. Radiat. Transfer* **33**, 521–532 (1985).
17. L. D. Gray and S. S. Penner, Approximate band absorption calculation for methane, *J. Quant. Spectrosc. Radiat. Transfer* **5**, 611–620 (1965).

18. R. Siegel and J. R. Howell, *Thermal Radiation Heat Transfer* (2nd Edn) p. 769. Hemisphere, Washington, DC (1981).
19. J. D. Felske and C. L. Tien, Wide band characterization of the total band absorptance of overlapping infrared gas bands, *Combust. Sci. Technol.* **11,** 111–117 (1975).
20. S. S. Penner and P. Varanasi, Effect of (partial) overlapping of spectral lines on the total emissivity of H_2O–CO_2 mixtures ($T \geqslant 800$ K), *J. Quant. Spectrosc. Radiat. Transfer* **6,** 181–192 (1966).
21. F. R. Steward and Y. S. Kocaefe, Total emissivity and absorptivity models for carbon dioxide, water vapor and their mixtures, *Proceedings of the Eighth Heat Transfer Conference* (Edited by C. L. Tien, C. V. Carey and S. Ferrel), pp. 735–740. Hemisphere, Washington, DC (1986).
22. R. M. Goody, A statistical model for water vapour absorption, *Quart. J. R. Met. Soc.* **78,** 165–169 (1952).
23. R. M. Goody, *Atmospheric Radiation*. Oxford Clarendon Press, Oxford (1964).
24. S. H. Chan and C. L. Tien, Total band absorptance of non-isothermal infrared-radiating gases, *J. Quant. Spectrosc. Radiat. Transfer* **9,** 1261–1271 (1969).
25. D. K. Edwards and S. J. Morizumi, Scaling of vibration-rotation band parameters for non-homogeneous gas radiation, *J. Quant. Spectrosc. Radiat. Transfer* **10,** 175–188 (1970).
26. T. K. Kim, J. A. Menart and H. S. Lee, Non-gray radiative gas analysis using the S-N discrete ordinate method, *ASME J. Heat Transfer* **113,** 946–952 (1991).
27. T. H. Song and R. Viskanta, Development and application of a spectral group model to radiation heat transfer, ASME paper no. 86-WA/HT-36, 1–9 (1986).
28. T. H. Song, Comparison of engineering models of non-gray behavior of combustion products, *Int. J. Heat Mass Transfer* **36,** 3975–3982 (1993).
29. M. K. Denison, A spectral line based weighted-sum of gray gases model for arbitrary RTE solvers, Ph.D. thesis, Brigham Young University (1994).
30. N. Lallemant and R. Weber, Evaluation of seven approximate emissivity models for CFD modelling of non-luminous flames, *37th EUROTHERM Symposium*, pp. 109–124 (1993).
31. A. Soufiani and E. Djavdan, A comparison between weighted sum of gray gases and statistical narrow-band radiation models for combustion applications, *Combust. Flame* **97,** 240–250 (1994).
32. D. K. Edwards, Numerical methods in radiation heat transfer. In *Proceedings of the Second Symposium on Numerical Properties and Methodologies in Heat Transfer* (Edited by T. M. Shih), pp. 479–496. Hemisphere, Washington, DC (1983).
33. R. J. Hall and A. Vranos, Efficient calculations of gas radiation from turbulent flames, *Int. J. Heat Mass Transfer* **37,** 2745–2750 (1994).